

# Mutation of Tn5 Transposase $\beta$ -Loop Residues Affects All Steps of Tn5 Transposition: The Role of Conformational Changes in Tn5 Transposition<sup>†</sup>

Mindy Steiniger,<sup>‡</sup> Jeremy Metzler, and William S. Reznikoff\*

Department of Biochemistry, University of Wisconsin—Madison, Madison, Wisconsin 53562

Received June 20, 2006; Revised Manuscript Received September 15, 2006

**ABSTRACT:** X-ray cocrystal structures of Tn5 transposase (Tnp) bound to its 19 base pair (bp) recognition end sequence (ES) reveal contacts between a  $\beta$ -loop (amino acids 240–260) and positions 3, 4, 5, and 6 of the ES. Here, we show that mutations of residues in this loop affect both *in vivo* and *in vitro* transposition. Most mutations are detrimental, whereas some mutations at position 242 cause hyperactivity. More specifically, mutations to the  $\beta$ -loop affect every individual step of transposition tested. Mutants performing *in vivo* and *in vitro* transposition less efficiently also form fewer synaptic complexes, whereas hyperactive Tnps form more synaptic complexes. Surprisingly, two hypoactive mutations, K244R and R253L, also affect the cleavage steps of transposition with a much more dramatic effect on the second double end break (DEB) complex formation step, indicating that the  $\beta$ -loop likely plays an important role in positioning the substrate DNA within the catalytic site. Finally, all mutants tested decrease efficiency of the final transposition step, strand transfer. A disparity in cleavage rate constants *in vitro* for mutants with changes to the proline at position 242 on transposons flanked by ESs differing in the orientation of the A–T base pair at position 4 allows us to postulate that P242 contacts the position 4 nucleotide pair. On the basis of these data, we propose a sequential model for end cleavage in Tn5 transposition in which the uncleaved PEC is not symmetrical, and conformational changes are necessary between the first and second cleavage events and also for the final strand transfer step of transposition.

Transposition is the process of moving DNA from one location to another. Tn5 is a well-studied composite, prokaryotic transposon consisting of two insertion sequences, IS50R and IS50L, flanked by 19 base pair (bp) inverted repeats termed outside ends (OEs) (1). IS50R encodes the transposase (Tnp), the only protein required for transposition in this system (2). Tn5 is mobilized using a cut-and-paste mechanism in which the transposon is completely removed from its original location before being inserted into a new DNA site (3).

Following translation, Tnp initially nonspecifically interacts with DNA but then localizes the OE by both inter and intramolecular transfer, possibly via a looping mechanism (Figure 1A; Adams, C. D., personal communication and ref 4 (4)). The OE bound Tnps then form a dimeric synaptic complex, the nucleoprotein complex required for catalysis (5–7). Following synapsis, cleavage occurs at one OE/flanking donor backbone (dbb) DNA junction (+1) followed by the other. First, a water molecule activated by  $Mg^{2+}$  attacks the phosphodiester backbone of one DNA strand at the +1 location, resulting in the generation of a 3' hydroxyl group (Figure 1B, column 1). This 3' hydroxyl group then attacks the opposite DNA strand creating a hairpin intermediate and releasing the dbb DNA (8). The synaptic complex

containing one cleaved end and one uncleaved end is referred to as the single end break complex (SEB) (8). The hairpin within the SEB is resolved by the nucleophilic attack of a second  $Mg^{2+}$ -activated water molecule. Cleavage of the DNA at the second OE/dbb junction then proceeds in the same fashion creating a blunt-ended transposon with free 3' hydroxyl groups (Figure 1B, column 2). The synaptic complex containing two cleaved DNA ends is referred to as the double end break (DEB) complex. Following cleavage, the DEB complex captures a nonspecific DNA target and inserts the transposon in a non-concerted fashion resulting in 9 bp duplications (Figure 1A and ref 9 (9)) (10, 11).

X-ray crystal structures have been solved for both DEB complexes containing OEs and a Tnp analogue, the inhibitor protein (Inh) (12–16). Interestingly, amino acids 240–260 are disordered in the absence of the OE (as in the Inh structure) but form a  $\beta$ -loop in the DEB complex structures (Figure 2). Various amino acids within this  $\beta$ -loop contact differing moieties of nucleotide pairs 3, 4, 5, and 6 of the OE, and the  $\beta$ -loop acts as a clamp, holding the DEB complex together.

Previously, a hyperactive 19 bp Tnp recognition end sequence (termed the mosaic end (ME)) was constructed, which differs from the OE at three positions: 4, 17, and 18 (17). The hyperactivity was shown to stem from the orientation of the adenine–thymine (A–T) bp at position 4 (15). When T was located on the non-transferred strand (Figure 2) closest to the  $\beta$ -loop, as in the ME, hyperactivity resulted. When the A–T base pair was in the opposite orientation, as in the wild type OE, synaptic complex

<sup>†</sup> This work was supported by NIH grant GM50692 to W.S.R. (M.S. and J.D.M.).

\* Corresponding author. Tel: (608) 262-3608. Fax: (608) 265-2603. E-mail: reznikoff@biochem.wisc.edu.

<sup>‡</sup> Current address: Lineberger Comprehensive Cancer Center, University of North Carolina at Chapel Hill, Chapel Hill, NC 27599.

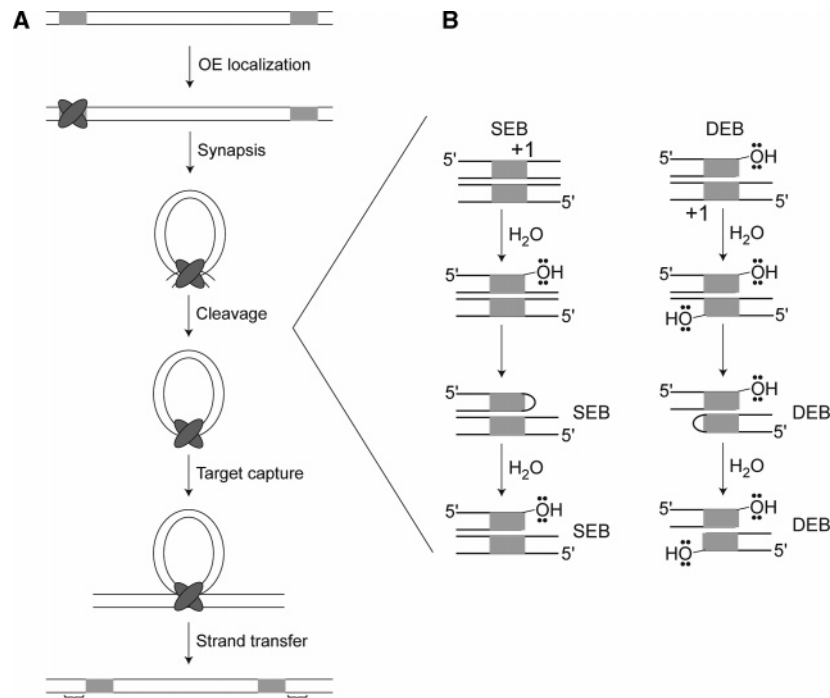


FIGURE 1: (A) Mechanism of Tn5 transposition. Tn5 Tnp initially interacts with DNA in a non-specific manner followed by OE localization via inter and intramolecular transfer. The OE bound Tnps then form a dimeric synaptic complex. Cleavage of the transposon from the flanking or donor backbone (dbb) DNA occurs within this complex by a two step sequential process (see B). Following cleavage, the double end break (DEB) complex captures a non-specific target and integrates the transposon resulting in 9 bp duplications. The Tnp is represented by a gray oval, and the OEs are shown as light gray rectangles. The 9 bp duplications are represented by { . (B) More detailed description of the cleavage step of Tn5 transposition. The cleavage site is marked with +1, and the Tnp has been omitted for clarity. First, a Mg<sup>2+</sup> activated water molecule attacks the phosphodiester backbone of the transferred strand (Figure 2) at +1 resulting in the formation of a 3' hydroxyl group. This 3' hydroxyl group then attacks the non-transferred strand (Figure 2) directly opposite of the initial nick, creating a hairpin intermediate. The resulting complex is referred to as the single end break (SEB) complex. The hairpin is resolved by attack of another Mg<sup>2+</sup> activated water molecule, completing cleavage at this end of the transposon. Cleavage at the second end occurs via the same mechanism resulting in the double end break (DEB) complex and is shown in the second column. The DEB complex is competent for target capture and strand transfer.

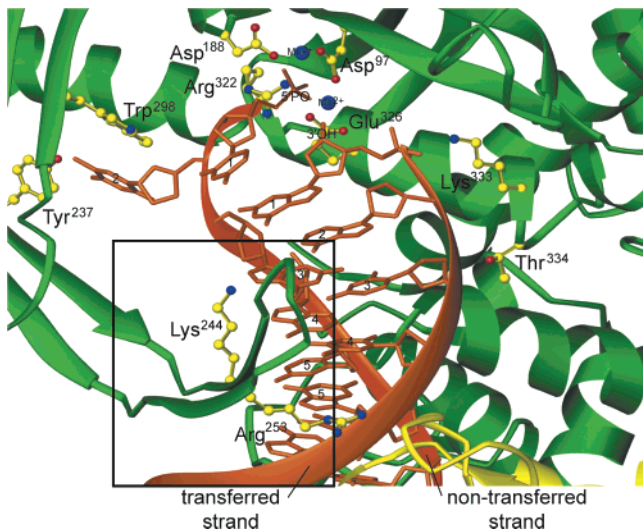


FIGURE 2: Magnified view of contacts between Tnp and bases 1–5 of the ES in the Tnp-ES cocrystal structure. The Tnp is represented in green ribbon format, whereas the DNA is shown in orange, and the base pairs are numbered appropriately. Catalytic triad residues Asp97, Asp188, and Glu326 together with other important amino acids are represented in yellow ball-and-stick format and are labeled. Transferred and non-transferred DNA strands are also labeled. The Tnp β-loop contacting bases 3–5 of the ES is accented with a black box.

formation was much less efficient (15). Interestingly, in X-ray crystal structures of the DEB complex containing the OE or

the ME, no contacts are observed between the Tnp β-loop and the base pair at position 4 (16). This led us to conclude that the contact between Tnp and the ME necessary for hyperactivity must occur at a transposition step preceding that observed in the crystal structures.

To investigate this further, mutations were made to residues in the β-loop, and their affect on Tn5 transposition was tested both *in vivo* and *in vitro*. Also, the individual steps of transposition, synaptic complex formation, cleavage, and strand transfer, were examined more rigorously using only purified Tnp, small fluorescently labeled oligonucleotides containing either the OE or the ME, Mg<sup>2+</sup>, and a target DNA to reconstitute these steps of Tn5 transposition *in vitro*.

From these experiments, we learned that contacts between residues in the β-loop and the recognition end sequence (ES, either the OE or ME) are important for multiple steps in Tn5 transposition. More specifically, mutations to K244 not only affect synaptic complex formation but also slow catalysis and strand transfer. The mutation of R253 to a leucine has a similar affect. In addition, mutations to K244 and R253 have more severe effects on the second DNA cleavage event compared to those the preceding first DNA cleavage event. Changing Q243 to a glutamate or R256 to a leucine not only decreases synaptic complex formation efficiency but also alters the type of complexes observed. Two mutants with changes at amino acid P242, P242A Tnp, and P242G Tnp are hyperactive *in vivo* and *in vitro* and form more synaptic complexes than the control Tnp. Interest-

ingly, these mutants perform the strand transfer step of transposition less efficiently, indicating that increased synaptic complex formation must more than compensate for defects in later steps of transposition. Because the  $\beta$ -loop is not in the catalytic core and, therefore, cannot directly affect the catalytic steps of transposition, we suggest that conformational changes necessary for catalysis require interactions between the Tnp  $\beta$ -loop and the ES. Finally, additional mutations were made at P242, and all were found to be hyperactive *in vitro* with a ME flanked transposon. Conversely, only P242A Tnp, P242G Tnp, P242L, and P242V were found to be hyperactive on an OE flanked transposon. These data indicate that P242 may contact position 4 of the ES. A model encompassing these observations will be presented.

## EXPERIMENTAL PROCEDURES

**Site Directed Mutagenesis.** All DNA manipulations were performed in *Escherichia coli* strain DH5 $\alpha$  (18). All DNA polymerase chain reaction (PCR) primers were obtained from Integrated DNA Technologies (IDT). All mutant Tnp constructs contain hyperactive E54K and L372P mutations (19, 20) and the M56A mutation (21).

All point mutants were constructed by overlap PCR (22). Bases corresponding to amino acids 140–358 were amplified from pRZ10300 (5) by PCR using Pfu polymerase and internal mismatched primers containing the point mutation. The external primers included *NotI* and *NheI* restriction sites in the Tnp gene. The PCR products were digested with *NotI* and *NheI* and cloned into the large *NotI*–*NheI* fragment of pGRYTB35 (8). All proteins used in this study were purified to homogeneity at the same time using the same previously described method (4). It should be noted that the protein referred to as Tnp throughout this article contains the above mentioned hyperactive E54K and L372P mutations as well as the M56A mutation.

**Transposition Assay *in Vivo*.** The *in vivo* papillation assay was performed essentially as described (23). Plasmids expressing  $\beta$ -loop mutant Tnps (or the control Tnp) were transformed into an *E. coli* strain containing a transposon with a promoterless *lacZ* gene. These cells were then plated on minimal media containing X-gal (Sigma), phenyl  $\beta$ -D-galactoside (Sigma), ampicillin (100  $\mu$ g/mL), and tetracycline (10  $\mu$ g/mL). Following overnight incubation at 37 °C, single colonies were replica plated onto these same plates so as to give each colony equal resources. Plates were then incubated for 3–5 days at 30 °C to allow the production of blue papilli. The number of papilli observed for each mutant Tnp was then qualitatively compared to that of the control Tnp to determine an approximate increase or reduction in activity. Photographs were taken following overnight incubation at 4 °C.

**Transposition Assay *in Vitro*.** The *in vitro* transposition assay was performed essentially as described (5). To assay Tnp activity on the mosaic end (ME), 12.5 nM pKJ4 (15) was incubated with 100 nM Tnp in 20 mM Hepes (pH 7.5), 100 mM potassium glutamate, and 10 mM magnesium acetate (MgAc) buffer at 37 °C. To assay Tnp activity on the outside end (OE), 12.5 nM (15) was incubated with 250 nM Tnp in transposition buffer at 37 °C. Timepoints were taken for varying lengths of time (depending on the activity

of the  $\beta$ -loop mutant) by adding 8  $\mu$ L of each reaction to 4  $\mu$ L of 1% SDS. Following completion of the time course, 4  $\mu$ L of 6X loading dye (30% glycerol, 0.25% bromophenol blue, and 0.25% xylene cyanol) was added, and the timepoints were electrophoresed on a 1.3% agarose gel followed by visualization of reaction products by ethidium bromide staining. This reaction was repeated three times for each mutant. The percentage of supercoiled substrate remaining at each timepoint was then quantitated using Total Lab software. These percentages were plotted versus time and fit to a single phase exponential decay equation

$$y = a \times e^{(-kx)} + b \quad (1)$$

where  $a$  = the amplitude,  $b$  = the plateau, and  $k$  = the observed *in vitro* transposition rate constant. Both the observed rate constant and the standard error of the rate were determined for each mutant using this fit.

**PEC Formation Assay.** Paired ends complex (PEC) formation with Tnp mutants was assayed essentially as described (15). Forty nanomolar fluorescently labeled 60-bp double stranded oligonucleotide containing the ME (sequence in ref 15 (15)) was incubated with 175 nM Tnp in 20 mM HEPES (pH 7.5) and 100 mM potassium glutamate for 1.5 h at 37 °C. The loading dye was added, and PECs were separated from unbound DNA by electrophoresis on a 7% native gel. Complexes were visualized using a Typhoon 9410 Variable Mode Imager.

**Cleavage Assay.** To examine cleavage for Tnp (control), K244R, R253L, P242A, P242G, P242V, and P242L Tnps, 40 nM fluorescently labeled 60-bp double stranded oligonucleotide containing the ME was incubated with 175 nM Tnp in 20 mM HEPES (pH 7.5) and 100 mM potassium glutamate for 1.5 h at 37 °C. A 20  $\mu$ L aliquot was then removed before adding MgAc to a final concentration of 10 mM. Then, 20  $\mu$ L timepoints were taken from 45 s to 1 h and added to 5  $\mu$ L of cold gel loading dye. The cleavage products were electrophoresed on a 7% native polyacrylamide gel and visualized using a Typhoon 9410 Variable Mode Imager. The bands corresponding to PECs, single end break (SEB) complexes, and double end break (DEB) complexes were quantitated relative to each other using Image Quant Total Lab Software and plotted versus time to visualize the effect of the mutations on DNA cleavage. The data corresponding to a decrease in PECs over time was fit with single-exponential decay eq 1. The data corresponding to the variation in both SEB and DEB complexes over time were fit with a point-to-point spline.

**Strand Transfer Assay.** To examine strand transfer efficiency for Tnp (control), K244R, R253L, P242A, P242G, P242V, and P242L Tnps, 25 nM fluorescently labeled 40-bp double stranded oligonucleotide containing the ME but no donor backbone DNA (sequence in ref 15 (15)) was incubated with 150 nM Tnp in 20 mM HEPES (pH 7.5) and 100 mM potassium glutamate for 1.5 h at 37 °C to form post-cleavage PECs. A 20  $\mu$ L aliquot was then removed from each reaction and separated on a 7% native polyacrylamide gel to assess post-cleavage PEC formation for each mutant. To the remaining reaction, MgAc was added to a final concentration of 10 mM, and supercoiled pUC19 was added to 100 nM. Then, 10  $\mu$ L timepoints were removed from 0 to 24 h, added to 5  $\mu$ L of 1% SDS, and heated at 65 °C for

5 min. Agarose loading dye (5  $\mu$ L) was then added, and the timepoints were placed at  $-20$  °C. The two strand transfer products, single end strand transfer (SEST) and double end strand transfer (DEST) were separated together with the unreacted substrate by electrophoresis on a 2% agarose gel. Strand transfer products were then visualized using a Typhoon 9410 Variable Mode Imager and were quantitated using Image Quant Total Lab Software. The initial rate of strand transfer was then assessed by plotting the fluorescence units (FUs) corresponding to the DEST product versus time for the first 5–6 timepoints and fitting the data to a first-order polynomial

$$y = mx + b \quad (2)$$

where  $m$  = the slope and  $b$  = the  $y$ -intercept. In this case, the slope corresponds to the initial strand transfer rate constant for each Tnp.

## RESULTS

*Analysis of  $\beta$ -Loop Mutants in Vivo.* Previous cocrystal structures of Tn5 Tnp paired ends complexes (PECs) show a  $\beta$ -loop (amino acids 240–260) of Tnp contacting nucleotide pairs 3–5 of the recognition end sequence (ES) (13, 15, 16) (Figure 2). To understand the biological relevance of these interactions, mutations were made to several amino acids in this  $\beta$ -loop. The mutations were designed to study both Tnp–base specific contacts and Tnp–DNA phosphate backbone interactions. Also, each amino acid was only changed minimally so as to specifically determine the amino acid requirements at each position.

To measure the *in vivo* activity of each mutant, a papillation assay was performed (23). In this qualitative colorimetric assay, the ability of Tnp to transpose a promoterless *lacZ* gene flanked by outside ends (OEs) is assessed. When the Tnp expressed in trans can mobilize the transposon and insert it downstream of an active promoter in the correct reading frame and orientation,  $\beta$ -galactosidase is produced. This is observed as blue papilli among other *lacZ* minus *E. coli* when X-gal and phenyl  $\beta$ -D-galactoside are included in the media. The number of papilli corresponds to the activity level of Tnp.

This assay was performed for several  $\beta$ -loop mutants. Figure 3A shows the activity level of mutants found to be hypoactive compared to that of the Tnp control. The K244R mutation results in approximately 2-fold reduction in papilli formation, whereas the K244A mutation reduces papillation approximately 10-fold. The K244E mutation completely abolishes *in vivo* transposition. The removal of charge from the side chains of two arginine residues (253 and 256) causes an approximate 3-fold reduction in papillation for R253L Tnp and complete loss of activity for R256L Tnp. The Q243E mutation also causes the inactivation of Tnp.

Figure 3B shows the activity level of mutants at position 242, found to be hyperactive compared to that of the Tnp control. It should be noted that although the Tnp control seems less active in Figure 3B than in 3A, this is because of a shorter incubation time for the control in Figure 3B. The mutation of P242 to either alanine or glycine results in significant hyperactivity, whereas mutation to isoleucine or leucine results in only a marginal increase.

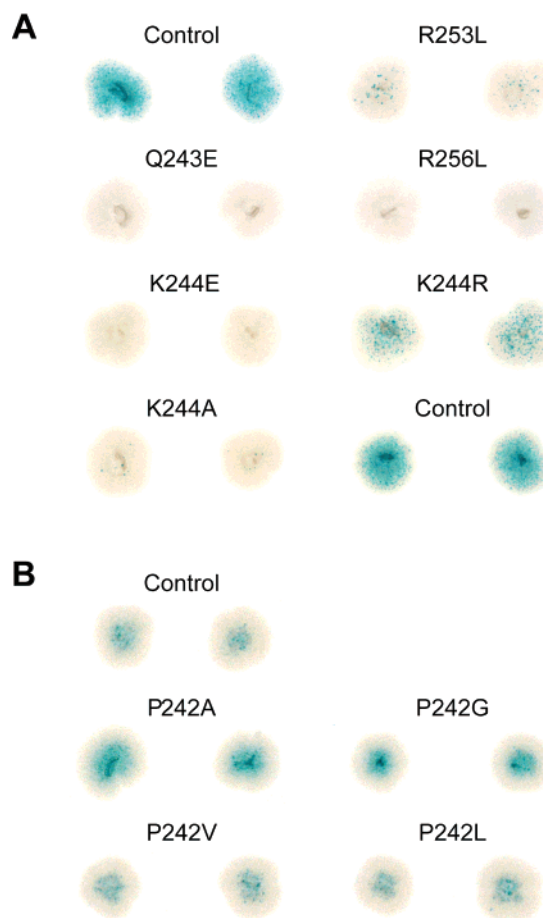
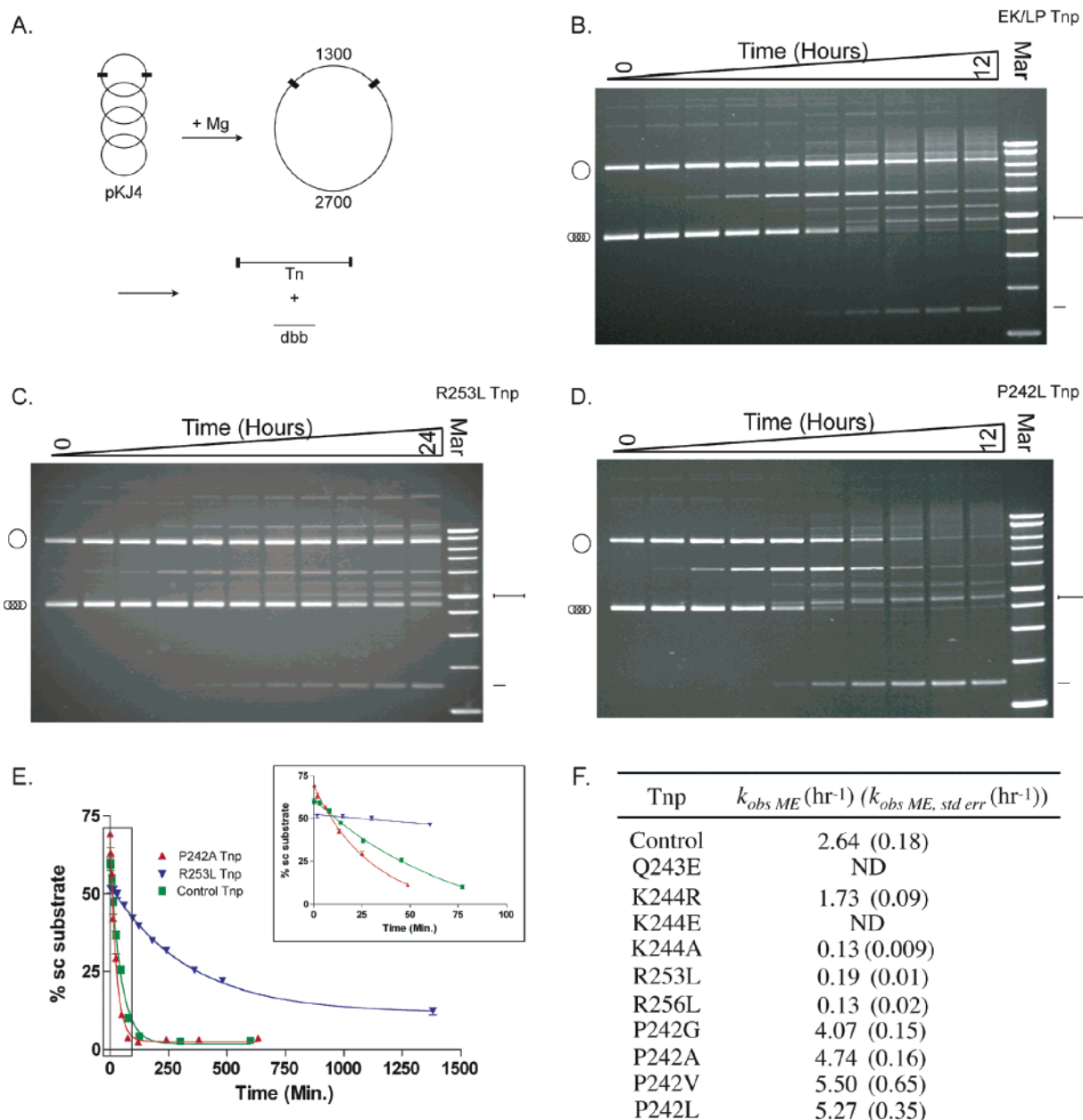


FIGURE 3: (A) Papillation assay showing transposition activity for hypoactive Tnps. The  $\beta$ -loop mutant Tnps (or control Tnp) were expressed in an *E. coli* strain with a promoterless *lacZ* gene flanked by outside ends (OEs). The Tnps move this transposon (Tn) to new locations in the genome with some frequency, and when the Tn is inserted in the proper orientation and reading frame,  $\beta$ -galactosidase is produced. When X-gal and a lactose analogue are included in the media, cells capable of  $\beta$ -galactosidase production appear as blue papilli. The total number of blue papilli in each colony indicates the activity level of the Tnp. The control Tnp, shown in both the top left and bottom right corners, causes enough transposition so that the entire colony appears blue. The R253L mutation causes an approximately 3-fold reduction in papillation, whereas the Q243E and R256L mutations completely abolish *in vivo* transposition. The K244R mutation causes an approximately 2-fold reduction in papillation, whereas the K244A mutation causes a 10-fold reduction. The K244E mutation completely abolishes *in vivo* transposition. (B) Papillation assay showing transposition activity for Tnps with mutations to P242. It should be noted that although the control Tnp, shown in the top left corner, seems less active than that in A, this is due to a shorter incubation time for these *E. coli*. Both P242A and P242G have approximately 2-fold more blue papilli than the control Tnp, indicating that these mutant Tnps are hyperactive. P242V and P242L have approximately the same number of papilli as that of the control Tnp.

*Analysis of  $\beta$ -Loop Mutants in Vitro.* To observe the *in vitro* activity of the  $\beta$ -loop mutants, purified Tnps were incubated with a supercoiled plasmid (pKJ4) containing a transposon (Tn) flanked by mosaic ends (MEs) in transposition buffer containing magnesium ( $Mg^{2+}$ ). A schematic of this reaction is shown in Figure 4A. Aliquots of the reactions were stopped at timepoints by the addition of SDS to denature the Tnp, and the reaction products were separated on an agarose gel. The control *in vitro* reaction with Tnp is



**FIGURE 4:** (A) Schematic of the *in vitro* transposition reaction. Supercoiled plasmid pKJ4 was incubated with either the control Tnp or  $\beta$ -loop mutant Tnps in buffer containing  $Mg^{2+}$ . Over time, this results in nicking of pKJ4 followed by cleavage of the plasmid into transposon (Tn) and donor backbone (dbb) reaction products. The Tnp end sequences (ESes) are shown as black rectangles. (B) Twelve hour *in vitro* transposition time course for the control Tnp. The supercoiled pKJ4 substrate and all reaction products are labeled as in A. (C) Twenty-four hour *in vitro* transposition time course for R253L Tnp. The supercoiled pKJ4 substrate and all reaction products are labeled as in A. This reaction is shown as an example of the hypoactive  $\beta$ -loop mutant Tnps. (D) Twelve hour *in vitro* transposition time course for P242L Tnp. The supercoiled pKJ4 substrate and all reaction products are labeled as in A. This reaction is shown as an example of the hyperactive  $\beta$ -loop mutant Tnps. (E) Percent supercoiled pKJ4 quantitated at each timepoint for each reaction. These percents were then plotted versus time and fit to an exponential decay equation to determine the observed cleavage rate constant,  $k_{obs}$ . Here, the data and fits for the control Tnp (green), R253L Tnp (purple), and P242L Tnp (red) are shown. The inset shows magnification of timepoints 0–75 min. (F)  $k_{obs}$  for each  $\beta$ -loop mutant together with the standard error of each fit.

shown in Figure 4B. An example of an *in vitro* transposition reaction with a hypoactive Tnp is shown in Figure 4C (R253L Tnp), whereas an example with a hyperactive Tnp (P242L Tnp) is shown in Figure 4D.

To quantitate the effects of the  $\beta$ -loop mutations, the percentage of supercoiled substrate pKJ4 at each timepoint was calculated and plotted versus time. These data were then fit to an exponential equation to obtain the observed reaction rate constant ( $k_{obs}$ ). Figure 4E shows the analysis of the control Tnp, P242L Tnp, and R253L Tnp. The  $k_{obs}$  for each

$\beta$ -loop mutant is reported in Figure 4F together with the standard error of each measurement. All hypoactive or inactive *in vivo* transposition mutants show either no detectable (ND) *in vitro* activity (Q243E Tnp and K244E Tnp) or reduced *in vitro* activity (K244R Tnp, K244A Tnp, R253L Tnp, and R256L Tnp) compared to that of the control Tnp. These results correlate well with *in vivo* results, even though a ME flanked transposon was used for the *in vitro* experiment. All mutations to the P242 residue were hyperactive compared to the Tnp control, but the alanine, valine,

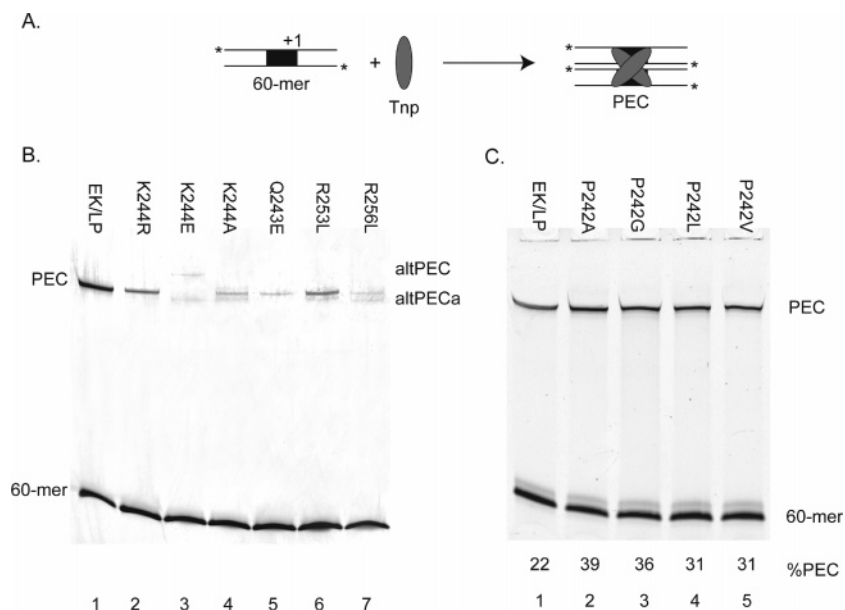


FIGURE 5: (A) Schematic of paired ends complex (PEC) formation. A 60 bp fluorescently labeled, ES-containing oligonucleotide was incubated with Tnp to form PECs. The fluorescent labels at the 5' end of each oligonucleotide are represented with \*. The 19 bp Tnp ES is shown as a black rectangle. The Tnp cleavage site at the Tn/dbb junction is marked with a +1. (B) PEC formation with the control Tnp and the hypoactive  $\beta$ -loop mutants. PECs and the unshifted substrate oligonucleotide are marked. Some mutants form additional PECs, marked with altPEC and altPECa. (C) PEC formation with the control Tnp and the hyperactive P242 mutants. PECs and the unshifted substrate oligonucleotide are marked. The percent DNA contained in PECs is shown for each mutant.

and leucine substitutions were significantly more hyperactive than the glycine mutation (compare 4.74, 5.10, and 5.27  $\text{h}^{-1}$  to 4.07  $\text{h}^{-1}$ ). This *in vitro*  $k_{\text{obs}}$  rate constant trend does not correlate with the previously discussed *in vivo* observations. This phenomenon will be explored later on in this article. It should be noted that  $k_{\text{obs}}$  corresponds to the loss of substrate and not to the creation of reaction products. However, an analysis of the percentage of donor backbone (dbb, see Figure 4) increase over time shows a similar  $k_{\text{obs}}$  trend for all mutants tested (data not show).

**Paired Ends Complex (PEC) Formation with the  $\beta$ -Loop Mutants.** Mutations to the Tn5 Tnp  $\beta$ -loop affect both *in vivo* Tnp activity and *in vitro* transposition rate constants. We next wanted to define which steps of the Tn5 transposition mechanism are affected by these mutations. To determine if the synaptic complex formation step is altered, paired ends complex (PEC) formation was assessed with the  $\beta$ -loop mutants. A PEC consists of two 19 bp recognition ES-containing oligonucleotides and two Tnp molecules and is analogous to the synaptic complex (7). Each mutant Tnp was incubated with an ME-containing oligonucleotide in transposition buffer. A schematic of this reaction is shown in Figure 5A. To visualize the PECs, the reactions were separated on a native gel, where PECs are shifted compared to the unbound oligonucleotide.

PEC formation with the hypoactive Tnp mutants is shown in Figure 5B. All hypoactive  $\beta$ -loop mutant Tnps formed PECs except for K244E Tnp, and the abundance of PECs formed by each mutant qualitatively corresponds to both the *in vivo* and *in vitro* activity levels. K244R and R243L cause some reduction in PEC formation, whereas K244A, Q243E, and R256L cause a significant reduction in PECs. Additionally, K244E Tnp forms the newly characterized altPEC containing two Tnps and two ESs but in a differing conformation than that of the PEC (Adams, C. D., personal communication), and K244E Tnp, R253L Tnp, and R256L

Tnp form an uncharacterized altPEC, termed the altPECa, which migrates more quickly than the PEC. From these data, we conclude that the hypoactive  $\beta$ -loop mutants have a defect in PEC formation and form alternative complexes with the ES-containing oligonucleotide.

Representative data for PEC formation with four hyperactive Tnp mutants is shown in Figure 5C. The efficiency of this reaction is measured by the percent PEC formation for each mutant, which is defined as the amount of ES-containing oligonucleotide in PECs divided by the total DNA in each reaction. This value is shown below the lane corresponding to each mutant.

The control Tnp complexed 22% of the substrate oligonucleotide. All of the hyperactive mutants tested formed more PECs than the control with the P242A mutation Tnp having the most dramatic effect, shifting 39% of the substrate DNA. P242G also increased PEC formation approximately 1.6-fold, resulting in 35% PEC formation. The P242L and P242V mutations had less of an effect, resulting in a 1.4-fold increase in PEC formation. From these data, we conclude that the hyperactive P242 mutants form more PECs than the control Tnp.

**Cleavage with the  $\beta$ -Loop Mutants.** All mutations to the Tn5 Tnp  $\beta$ -loop affect synaptic complex formation. Next, we wanted to determine if these mutations also perturb the cleavage steps of transposition. Four hyperactive  $\beta$ -loop mutants and the K244R and R253L hypoactive Tnps were incubated with an ME-containing oligonucleotide to form PECs. None of the other hypoactive Tnps formed enough PECs to assess the cleavage step of transposition.  $\text{Mg}^{2+}$  was then added to induce cleavage of the oligonucleotide at the transposon (Tn)/donor backbone (dbb) junction (+1), resulting in single end break (SEB) and double end break (DEB) complexes. A schematic of this reaction is shown in Figure 6A. Following the addition of  $\text{Mg}^{2+}$ , aliquots were removed over time and visualized on native polyacrylamide gels,

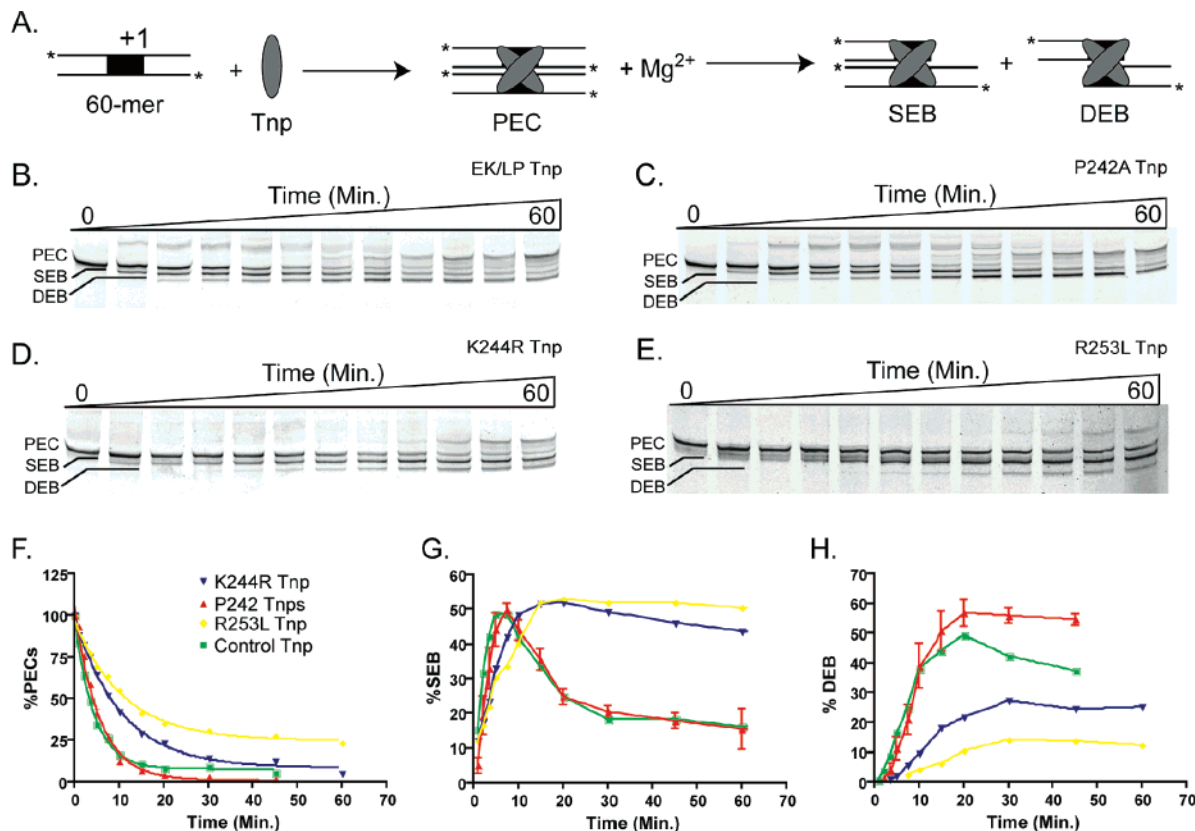


FIGURE 6: (A) Schematic of the cleavage reaction. First, PECs are formed as shown in Figure 5. Upon the addition of  $Mg^{2+}$  to these complexes, Tnp cleaves the dbb from the Tn, resulting first in a single end break (SEB) complex and, subsequently, in a double end break (DEB) complex. (B) Cleavage reaction for the control Tnp. Timepoints were taken from 0 to 60 min. PECs, SEB complexes, and DEB complexes are labeled. (C) Cleavage reaction for P242A Tnp. This reaction is representative of all hyperactive  $\beta$ -loop mutants. Timepoints were taken from 0 to 60 min. PECs, SEB complexes, and DEB complexes are labeled. (D) Cleavage reaction for K244R Tnp. Timepoints were taken from 0 to 60 min. PECs, SEB complexes, and DEB complexes are labeled. (E) Cleavage reaction for R253L Tnp. Timepoints were taken from 0 to 60 min. PECs, SEB complexes, and DEB complexes are labeled. (F) Amount of DNA present in PECs at each timepoint calculated as a percent of the total DNA in PECs, SEB complexes, and DEB complexes at each timepoint. These percent PECs were then plotted versus time and fit to an exponential equation. Data corresponding to the control Tnp is shown in green. The decrease in percent PECs over time was found to be similar for all hyperactive P242 mutants (data not shown). Therefore, the data for these Tnps, shown in red, were combined with variation from the mean being represented with error bars. The data corresponding K244R Tnp is shown in purple, whereas the data for R253L is shown in yellow. (G) Amount of DNA present in SEB complexes at each timepoint calculated as a percent of the total DNA in PECs, SEB complexes, and DEB complexes at each timepoint. These percent SEB complexes were then plotted versus time and fit with a spline. The increase and then decrease of percent SEB complexes over time was found to be similar for the hyperactive P242 mutants (data not shown). Therefore, the data for these Tnps, shown in red, were combined with variation from the mean being represented with error bars. Colors corresponding to other Tnps are as in F. (H) Amount of DNA present in DEB complexes at each timepoint calculated as a percent of the total DNA in PECs, SEB complexes, and DEB complexes at each timepoint. These percent DEB complexes were then plotted versus time and fit with a spline. The increase and then plateau of percent DEB complexes over time was found to be similar for the hyperactive P242 mutants (data not shown). Therefore, the data for these Tnps, shown in red, were combined with variation from the mean being represented with error bars. Colors corresponding to other Tnps are as in F.

where the SEB and DEB complexes migrate more slowly than PECs. Figure 6B shows a representative cleavage time course corresponding to the control Tnp. Figure 6C shows a representative cleavage time course performed with P242A Tnp. Figure 6D corresponds to K244R Tnp, whereas Figure 6E represents R253L Tnp. The percent substrate oligonucleotide in PECs, SEB complexes, and DEB complexes at each timepoint was determined relative to the total amount of substrate oligonucleotide contained in these three complexes. These percentages were then plotted versus time so as to qualitatively compare the effect of these  $\beta$ -loop mutations on the cleavage steps of transposition. Figure 6F shows the decrease in percent PECs for the  $\beta$ -loop mutants, Figure 6G shows fluctuations in percent SEB complexes, and Figure 6H shows the increase in percent DEB complexes for the  $\beta$ -loop mutants.

The analyses indicate that cleavage of the substrate oligonucleotide is similar for all hyperactive P242 mutants (data not shown). Therefore, these mutants are represented by the average percent PECs, SEB complexes, and DEB complexes at each timepoint together with error bars indicating one standard deviation from this average. The hyperactive P242 mutants behave in manner very similar to that of the Tnp control, having approximately the same rate of percent PEC decline (Figure 6F, compare red to green), percent SEB complex appearance and disappearance (Figure 6G, compare red to green) and percent DEB complex formation (Figure 6H, compare red to green, timepoints 0 through 10 min). The only significant difference between the hyperactive P242 mutants and the control lies in the fate of the DEB complexes. The hyperactive mutants make slightly more DEB complexes than the control (Figure 6H, compare red

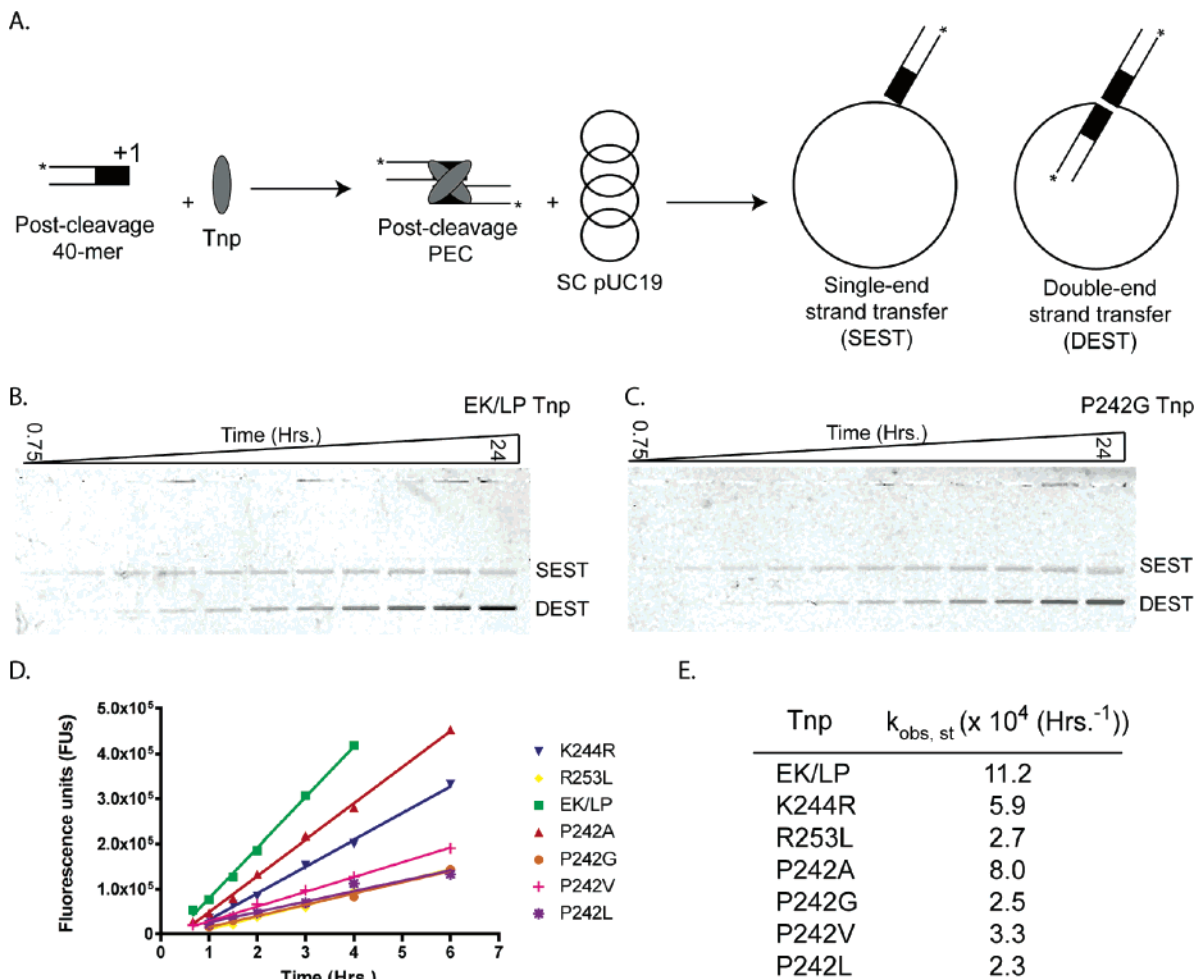


FIGURE 7: (A) Schematic of the strand transfer reaction. First, Tnp was incubated with a fluorescently labeled, 40 bp, ES-containing oligonucleotide lacking *dbb* DNA to form post-cleavage PECs. Supercoiled pUC19 was then added, and over the next 24 h, oligonucleotides in the post-cleavage PECs integrated into the supercoiled pUC19 resulting in transfer of the fluorescent label to the pUC19. A single end strand transfer (SEST) product appears first, followed by the double end strand transfer (DEST) product. (B) Strand transfer reaction with the control Tnp. Timepoints were taken from 45 min to 24 h. Both SEST and DEST products are labeled. (C) Strand transfer reaction with P242G Tnp. Because all  $\beta$ -loop mutants had decreased strand transfer activity, this reaction is representative of all  $\beta$ -loop mutants tested. Timepoints were taken from 45 min to 24 h. Both SEST and DEST products are labeled. (D) Amount of DEST product (in fluorescence units, FUs) at each timepoint determined for each mutant. FUs were then plotted versus time for timepoints 45 min through 6 h for all  $\beta$ -loop mutants and for timepoints 45 min through 4 h for the control Tnp. These points represent the linear portion of DEST product formation. These data were fit with a first-order polynomial to determine the observed strand transfer rate constant ( $k_{obs, st}$ ). Tnp is shown in green, K244R Tnp is shown in blue, R253L is shown in yellow, P242A is shown in red, P242G is shown in orange, P242V is shown in pink, and P242L is shown in purple. (E)  $k_{obs, st}$  calculated from the fits in D for each  $\beta$ -loop mutant or control Tnp.

to green at the 20 min timepoint), and the percent DEB complexes remains relatively constant from 20 min to 45 min for these mutants. Comparatively, the control Tnp produces the highest percent DEB complexes at 20 min, and then this reaction product slowly declines until the 45 min timepoint. This discrepancy reflects a decrease in the ability of the hyperactive P242 mutants to perform the next step of transposition, strand transfer. This will be explored further in the next sections.

Of the hypoactive  $\beta$ -loop mutants only two formed enough PECs to test the catalytic steps of Tn5 transposition, K244R Tnp and R253L Tnp (Figure 5B). Surprisingly, these mutants have deficiencies in catalysis in addition to defects in PEC formation. The percent PECs decrease more slowly for both K244R Tnp and R253L Tnp than that for the control Tnp (Figure 6F, compare blue and yellow to green). This slower decrease in percent PECs results in a lag in the appearance of SEB complexes for both mutants as compared to the

control (Figure 6G, compare blue and yellow to green, 0 through 15 min). Also, unlike the control Tnp, the rate of conversion of SEB complexes to DEB complexes is drastically reduced, resulting in a plateau of percent SEB complexes for the two hypoactive mutants (Figure 6G, blue and yellow 15 to 60 min) and a decreased rate of DEB complex appearance (Figure 6G, blue and yellow 0 to 20 min). Finally, the hypoactive mutants, like the hyperactive mutants, have a decreased ability to perform the next step of transposition, strand transfer. This is seen as a plateau in the percent DEB complexes (Figure 6H, blue and yellow, 20 to 60 min) and will be explored further in the next section. It should be noted that although both hypoactive mutations affect all catalytic steps, the R253L mutation causes a more severe defect than the K244R mutation.

*Strand Transfer with the  $\beta$ -Loop Mutants.* To determine if the  $\beta$ -loop mutations affect the last step of Tn5 transposition, strand transfer, post-cleavage PECs were first assembled

Table 1: Observed Catalytic Rate Constants ( $k_{\text{obs}}$ ) for  $\beta$ -Loop Mutants on ME- and OE-Containing Substrates

Tnp	$k_{\text{obs ME}} (\text{h}^{-1})$ ( $k_{\text{obs ME, std err}} (\text{h}^{-1})$ )	fold difference	$k_{\text{obs OE}} (\text{h}^{-1})$ ( $k_{\text{obs OE, std err}} (\text{h}^{-1})$ )	fold difference
control	2.64 (0.18)		0.79 (0.03)	
P242G	4.07 (0.15)	1.5	2.50 (0.10)	3.2
P242A	4.74 (0.16)	1.8	2.52 (0.14)	3.2
P242L	5.27 (0.35)	2.0	1.56 (0.07)	2.0
P242V	5.10 (0.13)	1.9	1.42 (0.06)	1.8
p242I	5.50 (0.65)	2.1	0.93 (0.03)	1.2
P242F	3.46 (0.12)	1.4	0.58 (0.03)	0.7
P242Y	4.52 (0.13)	1.7	0.60 (0.04)	0.8
P242D	5.53 (0.18)	2.1	0.55 (0.03)	0.7

with an oligonucleotide containing the ES but lacking dbb DNA. These complexes were incubated with supercoiled pUC19 DNA, where the oligonucleotides were incorporated into pUC19, resulting in single end and double end strand transfer products. See Figure 7A for a schematic of this reaction. Figure 7B shows the reaction for the control Tnp, whereas Figure 7C shows the reaction for P242G Tnp. The fluorescence units corresponding to the double end strand transfer (DEST) product were quantitated and plotted versus time for timepoints 0.75 through 6 h (or 0.75 through 5 h for EK/LP Tnp) (Figure 7D). These timepoints represent the linear portion of an exponential curve. The slope of each line is the observed initial DEST rate constant ( $k_{\text{obs, st}}$ ) for each  $\beta$ -loop mutant.

All  $\beta$ -loop mutants tested had a reduced  $k_{\text{obs, st}}$  compared to that of the control Tnp (Figure 7E). The P242A mutation had the least detrimental effect, showing only a 1.4-fold decrease in  $k_{\text{obs, st}}$ . The K244R mutation also had minimal effect, reducing  $k_{\text{obs, st}}$  1.9-fold. The remaining mutations, P242V, R253L, P242G, and P242L, reduced  $k_{\text{obs, st}}$  between 3.4- and 4.9 fold.

*P242 May Make a Base Specific Contact to Position 4 of the ES.* In the Tn5 Tnp-ES cocrystal structures, P242 is in close proximity to position 4 of the ES, but it does not actually contact any base. If thymine is present on the non-transferred strand (Figure 2) at position 4, hyperactivity resulting from more efficient synaptic complex formation is observed. To determine if a contact between the C5-methyl group (C5-Me) on the non-transferred strand thymine at position 4 (T4) of the ES and P242 may be responsible for the aforementioned hyperactivity, additional mutants were constructed (P242I, P242F, P242Y, and P242D). Following purification, each mutant was incubated with both a supercoiled substrate having a Tn flanked by MEs and a supercoiled substrate having a transposon with OEs in transposition buffer containing  $\text{Mg}^{2+}$ , and the observed reaction rate constant ( $k_{\text{obs}}$ ) for each P242 mutant was calculated. These reactions are similar to those seen in Figure 4.  $k_{\text{obs}}$  was determined for both ME and OE flanked Tns because the ME has a thymine on the non-transferred strand at position 4, whereas the OE has an adenine at this position.  $k_{\text{obs}}$  on the OE flanked Tn was also determined for the previously constructed P242 mutants (P242A, P242G, P242L, and P242V).  $k_{\text{obs}}$  for each reaction, the standard error of  $k_{\text{obs}}$ , and the fold difference between each mutant  $k_{\text{obs}}$  and the control  $k_{\text{obs}}$  are listed in Table 1.

All additional P242 mutant Tnps metabolized the ME flanked substrate faster than the control Tnp, with a fold difference in  $k_{\text{obs}}$  ranging from 1.4 to 2.1. Surprisingly, OE

flanked Tn catalysis did not follow this trend. P242G Tnp and P242A Tnp have a 3.2-fold larger  $k_{\text{obs}}$  than the control Tnp. This is approximately 2-fold greater than the hyperactivity seen on the ME flanked Tn. P242L Tnp and P242V Tnp also show hyperactivity on a Tn flanked with OEs, but the activity level is comparable to the hyperactivity of these mutants on a ME flanked Tn. The  $k_{\text{obs}}$  values for both mutants are approximately 2-fold greater on both ME and OE flanked Tns. Finally, the P242I Tnp shows only a minimal increase in  $k_{\text{obs}}$  on an OE flanked Tn, whereas P242F Tnp, P242Y Tnp, and P242D Tnp are actually less active on an OE flanked Tn than the control Tnp. The differences in rate constants on OE and ME flanked Tns allow us to formulate a model about Tnp interaction with position 4 of the ES. The details of this model will be presented in the Discussion section.

## DISCUSSION

*Contacts between a Tn5 Tnp  $\beta$ -Loop (Residues 240–260) and the ES Are Important for in Vivo and in Vitro Transposition.* Experiments *in vivo* and *in vitro* conclusively show that mutations to residues Q243, K244, R253, and R256 are detrimental to transposition.

The side chain of K244 approaches the position 3 non-transferred strand guanine but does not actually contact the base in the ES-Tnp cocrystal structure (16). When this residue is changed to an arginine, the guanidino group causes an approximately 60% reduction in transposition *in vivo* and *in vitro*. When all positive charge is removed by replacing the lysine with an alanine, transposition is reduced 90–95% both *in vivo* and *in vitro*. Finally, when the positively charged lysine is substituted with a negatively charged residue, a glutamate, all *in vivo* and *in vitro* transposition activity is lost. These data indicate that a base specific contact requiring a positively charged side chain is made between the residue at position 244 and the position 3 non-transferred strand guanine during Tn5 transposition. This is despite the fact that the precleaved ES-Tnp cocrystal structure fails to show such a contact (16). Perhaps the contact would be obvious if we had structural information on other steps in the transposition process.

Q243 makes a base specific contact to the position 6 transferred strand adenine in the ES-Tnp cocrystal structure. When this residue is changed, to a glutamate, all transposition activity is abolished. These data indicate that contact between the amide side chain of glutamine and the ES position 6 transferred strand base is essential for Tn5 transposition.

Mutations were also made to  $\beta$ -loop residues near the ES phosphate backbone in the ES-Tnp cocrystal structure. The guanidino group of R253 bridges ES phosphates between transferred strand bases 4 and 5. When this residue is changed to a leucine, therefore removing all positive charge, transposition is reduced approximately 90% both *in vivo* and *in vitro*. When the same mutation is made to R256, whose side chain nearly contacts the phosphate of non-transferred strand base 3 in the Tnp-ES cocrystal structure, transposition is undetectable *in vivo* and 95% reduced *in vitro*. These data indicate that contacts between positively charged residues in the  $\beta$ -loop and phosphates in the DNA backbone of the ES are integral for Tn5 transposition.

Although we postulate that these residues specifically contact the ES, disruption of electrostatic interactions can

have relatively long-range effects. Therefore, the absence of positive charges may cause disruption of other side chain–DNA interactions or general misalignment of the protein with the DNA phosphate backbone.

Finally, several mutations were made to P242. This residue does not contact any part of the ES in the ES-Tnp cocrystal structure (16). Therefore, we were surprised that changing the proline to either alanine or glycine caused hyperactive transposition *in vivo* and *in vitro*. Interestingly, when P242 was changed to valine or leucine, no hyperactivity was observed *in vivo*, but both mutant Tnps were hyperactive *in vitro*. This discrepancy reflects the difference in activity of the P242V and the P242L Tnps on OE versus ME flanked transposons and will be explored in much greater detail later in the discussion. We hypothesize that P242A Tnp and P242G Tnp are hyperactive because exchange of an imino group for an amino group causes increased flexibility of the  $\beta$ -loop and favorable base specific contacts between the amino acid at position 242 and the non-transferred strand base at position 4 of the ES. This will be discussed further in future publications.

*Mutations to the Tn5 Tnp  $\beta$ -Loop Affect Every Step of the Transposition Mechanism.* The  $\beta$ -loop mutant Tnps discussed in this article were constructed on the basis of the ES-Tnp cocrystal structure with the hypothesis that changing these residues would affect synaptic complex formation. Many mutations to  $\beta$ -loop residues caused decreased PEC formation, whereas mutations to position 242 caused increased PEC formation (Figure 5). These data indicate that the  $\beta$ -loop does indeed play an important role in PEC formation.

Surprisingly, when R253L Tnp and K244R Tnp were assayed for the cleavage (Figure 6) step of transposition, both were found to have defects in single end break (SEB) and double end break (DEB) complex formation with a much more dramatic effect on DEB formation (Figure 6H). These results were surprising because the  $\beta$ -loop is not near the active site in the ES-Tnp cocrystal structure and, therefore, cannot have a direct effect on catalysis. Even more surprising was the effect of the  $\beta$ -loop mutations on the final step of transposition, strand transfer. Every  $\beta$ -loop Tnp was less efficient than the control Tnp at this transposition step (Figure 7). The above data require changes to the current Tn5 transposition model. This changed model will be presented at the end of this article.

*Residue P242 Contacts the Thymine at Position 4 of the ES.* Previous data indicate that the hyperactivity of the ME ES is due to a contact between Tnp and the C5-methyl group (C5-Me) of the non-transferred strand (Figure 2) position 4 thymine (T4) (15). The observed catalytic rate constants ( $k_{\text{obs}}$ ) for eight position 242 mutant Tnps on both the wild-type outside ES (OE) and the ME are reported in Table 1. These data show that every P242 mutant Tnp is hyperactive for *in vitro* transposition with a ME flanked transposon and that  $k_{\text{obs}}$  is between 1.4- and 2.1-fold greater for these mutants than for the control Tnp. Contrastingly, four of the eight P242 mutants (P242I, P242F, P242Y, and P242D) have approximately the same or even less activity than that of the control Tnp on an OE flanked transposon, and more significant hyperactivity is seen for P242G and P242A Tnps under these conditions with  $k_{\text{obs}}$  being about 3.2-fold greater for these mutants. Because the only significant difference between the ME and the OE (as it pertains to these data) is

in the orientation of the A–T base pair at position 4, we conclude that the differences in  $k_{\text{obs}}$  (ME) and  $k_{\text{obs}}$  (OE) indicate that P242 contacts this base pair.

At position 4 of the ME, the C5-Me of the non-transferred strand T4 protrudes into the major groove near P242. Mutant Tnps with larger nonpolar side chains (L, V, and I) are slightly more hyperactive than residues with smaller nonpolar side chains (G and A) on this ES. This implies that leucine, valine, and isoleucine have side chains large enough to contact the C5-Me, whereas the methyl side chain of alanine and the hydrogen side chain of glycine are too small to interact with C5-Me. Therefore, P242L, P242V, and P242I are more hyperactive on the ME than P242A and P242G. Why then are P242A Tnp and P242G Tnp hyperactive on the OE? The non-transferred strand position 4 is occupied by an adenine (A4) in the OE. Because A4 is much larger than the T4 present in the ME, mutant Tnps with larger nonpolar side chains (L, V, and I) are sterically hindered when trying to interact with the OE. This causes a reduction in the observed hyperactivity compared to that of P242A and P242G Tnps.

Here, we also present evidence that PEC formation is more efficient for the P242 mutations on a substrate with the ME. These observations, taken together with the evidence of *in vitro* hyperactivity, allow us to propose that removing an imino acid from the base of the  $\beta$ -loop increases flexibility such that synaptic complex formation becomes more efficient. Unfortunately, this increased flexibility is not useful when the side chain of the amino acid at position 242 is large enough to be sterically hindered by the base at position 4 of the ES upon synaptic complex formation. This is the case for many of the P242 Tnps upon complex formation with the OE.

*New Model of Tn5 Transposition.* Observations presented in this article allow us to present a new model of Tn5 transposition. A crystal structure of a Tnp lacking the N-terminal 55 amino acids shows that the  $\beta$ -loop is disordered in the absence of DNA (12). Also, ES-Tnp cocrystal structures indicate that contacts between the  $\beta$ -loop and the ES are trans contacts or those that occur upon synaptic complex formation (13). Data presented here support these findings. All  $\beta$ -loop mutations tested cause either a reduction or an increase in PEC formation (Figure 4). As the synaptic complex forms, the  $\beta$ -loop interacts with residues 3–7 of the ES, and these contacts are important for maintaining the integrity of the complex. Because changes to residues that contact both the DNA phosphate backbone and specific bases have an effect, we propose that both types of contacts are important for synaptic complex formation.

As previously mentioned, the K244R and R253L mutations also have an effect on the catalytic steps of transposition. Interestingly, both SEB complex and DEB complex formation are slowed down with these Tnps, indicating that the  $\beta$ -loop likely plays an important role in positioning the substrate DNA within the catalytic site, but the effect on DEB complex formation is much more dramatic (Figure 6). Because the effect on DEB complex formation is proportionally greater than the effect on SEB formation, we propose that the uncleaved PEC is not symmetrical and that one ES is completely cleaved before a conformational change allows the cleavage of the other ES (Figure 1B). This model is consistent with the mechanism of Tn10, a closely related

transposon, transposition (24). Interestingly, the post-cleavage Tnp-ES cocrystal structures show a symmetrical dimer of Tnp bound ESs (13). Also, no accessory proteins such as IHF are required for Tn5 transposition. Therefore, the source of the asymmetry required for a sequential cleavage mechanism remains a mystery and requires further investigation.

Finally, how do mutations in a region distant from the active site affect all catalytic steps (cleavage and strand transfer) of Tn5 transposition? We (and others) have previously proposed that transposition must require significant conformational changes in the Tnp. These mutations and their effects on catalysis support this notion. If cleavage on the ES is sequential, as we now believe it is, then the conformational change required to initiate cleavage on the second ES must require K244 and R253 to appropriately contact the ES. Also, the conformational change needed to either capture or integrate into a target DNA must require very specific contacts between the  $\beta$ -loop and the ES.

In this article, we have shown the importance of contacts between the Tn5 Tnp  $\beta$ -loop and the ES for multiple steps of Tn5 transposition. The results of these experiments allow us to significantly modify our current model of Tn5 transposition to include a sequential cleavage step and a requirement for several Tnp conformational changes. These findings have broad implication to many transposition mechanisms.

#### ACKNOWLEDGMENT

We would like to thank Barb Shriver and Debbie Hug for media and reagent preparation.

#### REFERENCES

1. Johnson, R. C., and Reznikoff, W. S. (1983) DNA sequences at the ends of transposon Tn5 required for transposition, *Nature* 304, 280–282.
2. Johnson, R. C., and Reznikoff, W. S. (1984) Role of the IS50 R proteins in the promotion and control of Tn5 transposition, *J. Mol. Biol.* 177, 645–661.
3. Goryshin, I. Y., and Reznikoff, W. S. (1998) Tn5 in vitro transposition, *J. Biol. Chem.* 273, 7367–7374.
4. Steiniger, M., Adams, C. D., Marko, J. F., and Reznikoff, W. S. (2006) Defining characteristics of Tn5 Transposase non-specific DNA binding, *Nucleic Acids Res.* 34, 2820–2832.
5. Steiniger-White, M., and Reznikoff, W. S. (2000) The C-terminal alpha helix of Tn5 transposase is required for synaptic complex formation, *J. Biol. Chem.* 275, 23127–23133.
6. de la Cruz, N. B., Weinreich, M. D., Wiegand, T. W., Krebs, M. P., and Reznikoff, W. S. (1993) Characterization of the Tn5

- transposase and inhibitor proteins: a model for the inhibition of transposition, *J. Bacteriol.* 175, 6932–6938.
7. Bhasin, A., Goryshin, I. Y., Steiniger-White, M., York, D., and Reznikoff, W. S. (2000) Characterization of a Tn5 pre-cleavage synaptic complex, *J. Mol. Biol.* 302, 49–63.
  8. Bhasin, A., Goryshin, I. Y., and Reznikoff, W. S. (1999) Hairpin formation in Tn5 transposition, *J. Biol. Chem.* 274, 37021–37029.
  9. Reznikoff, W. S. (2003) Tn5 as a model for understanding DNA transposition, *Mol. Microbiol.* 47, 1199–1206.
  10. Mizuuchi, K., and Adzuma, K. (1991) Inversion of the phosphate chirality at the target site of Mu DNA strand transfer: evidence for a one-step transesterification mechanism, *Cell* 66, 129–140.
  11. Goryshin, I. Y., Miller, J. A., Kil, Y. V., Lanzov, V. A., and Reznikoff, W. S. (1998) Tn5/IS50 target recognition, *Proc. Natl. Acad. Sci. U.S.A.* 95, 10716–10721.
  12. Davies, D. R., Braam, L. M., Reznikoff, W. S., and Rayment, I. (1999) The three-dimensional structure of a Tn5 transposase-related protein determined to 2.9-Å resolution, *J. Biol. Chem.* 274, 11904–11913.
  13. Davies, D. R., Goryshin, I. Y., Reznikoff, W. S., and Rayment, I. (2000) Three-dimensional structure of the Tn5 synaptic complex transposition intermediate, *Science* 289, 77–85.
  14. Lovell, S., Goryshin, I. Y., Reznikoff, W. R., and Rayment, I. (2002) Two-metal active site binding of a Tn5 transposase synaptic complex, *Nat. Struct. Biol.* 9, 278–281.
  15. Steiniger-White, M., Bhasin, A., Lovell, S., Rayment, I., and Reznikoff, W. S. (2002) Evidence for “unseen” transposase–DNA contacts, *J. Mol. Biol.* 322, 971–982.
  16. Steiniger-White, M., Rayment, I., and Reznikoff, W. S. (2004) Structure/function insights into Tn5 transposition, *Curr. Opin. Struct. Biol.* 14, 50–57.
  17. Zhou, M., Bhasin, A., and Reznikoff, W. S. (1998) Molecular genetic analysis of transposase-end DNA sequence recognition: cooperativity of three adjacent base-pairs in specific interaction with a mutant Tn5 transposase, *J. Mol. Biol.* 276, 913–925.
  18. Sambrook, J., Fritsch, E. F., and Maniatis, T. (1989) *Molecular Cloning: A Laboratory Manual*, 2nd ed., Cold Spring Harbor Laboratory Press, Cold Spring Harbor, NY.
  19. Zhou, M., and Reznikoff, W. S. (1997) Tn5 transposase mutants that alter DNA binding specificity, *J. Mol. Biol.* 271, 362–373.
  20. Weinreich, M. D., Gasch, A., and Reznikoff, W. S. (1994) Evidence that the cis preference of the Tn5 transposase is caused by nonproductive multimerization, *Genes Dev.* 8, 2363–2374.
  21. Wiegand, T. W., and Reznikoff, W. S. (1992) Characterization of two hypertransposing Tn5 mutants, *J. Bacteriol.* 174, 1229–1239.
  22. Horton, R. M., Hunt, H. D., Ho, S. N., Pullen, J. K., and Pease, L. R. (1989) Engineering hybrid genes without the use of restriction enzymes: gene splicing by overlap extension, *Gene* 77, 61–68.
  23. Krebs, M. P., and Reznikoff, W. S. (1988) Use of a Tn5 derivative that creates lacZ translational fusions to obtain a transposition mutant, *Gene* 63, 277–285.
  24. Liu, D., Crellin, P., and Chalmers, R. (2005) Cyclic changes in the affinity of protein–DNA interactions drive the progression and regulate the outcome of the Tn10 transposition reaction, *Nuc. Acids Res.* 33, 1982–1992.

BI061227V